

Discovery of Nonpeptidic Small-Molecule AP-1 Inhibitors: Lead Hopping Based on a Three-Dimensional Pharmacophore Model

Keiichi Tsuchida,^{*,†} Hisaaki Chaki,[‡] Tadakazu Takakura,[†] Hironori Kotsubo,[‡] Tadashi Tanaka,[†] Yukihiro Aikawa,[‡] Shunichi Shiozawa,^{#,⊥} and Shuichi Hirono[§]

Discovery Laboratories and Research Laboratories, Toyama Chemical Co., Ltd., 4-1 Shimoookui 2-chome, Toyama 930-8508, Japan, Department of Rheumatology, Faculty of Health Science, Kobe University School of Medicine, 7-10-2 Tomogaoka, Suma-ku, Kobe 654-0142, Japan, Rheumatic Disease Division, Kobe University Hospital, 7-5-2 Kusunoki-cho, Chuo-ku, Kobe 650-0017, Japan, and School of Pharmaceutical Sciences, Kitasato University, 5-9-1 Shirokane, Minato-ku, Tokyo 108-8641, Japan

Received June 13, 2005

We designed and synthesized small-molecule activator protein-1 (AP-1) inhibitors based on a three-dimensional (3D) pharmacophore model that we had previously derived from a cyclic decapeptide exhibiting AP-1 inhibitory activity. New AP-1 inhibitors with a 1-thia-4-azaspiro[4.5]decane or a benzophenone scaffold, which inhibit the DNA-binding and transactivation activities of AP-1, were discovered using a “lead hopping” procedure. An additional investigation of the benzophenone analogues confirmed the reliability of the pharmacophore model, its utility to discover AP-1 inhibitors, and the potency of the benzophenone derivatives as a lead series.

Introduction

Activator protein-1 (AP-1) is a transcription factor that has a crucial role in cellular signal transduction, as it is responsible for the induction of a number of genes that are involved in cell proliferation, differentiation, and immune and inflammatory responses.^{1,2} It has been implicated in various diseases, such as rheumatoid arthritis.^{3,4}

AP-1 contains members of the Fos and Jun families, which form either Jun-Jun homodimers or Fos-Jun heterodimers and bind to the consensus DNA sequence 5'-TGAGTCA-3', which is known as the AP-1 binding site.¹ An investigation of the X-ray crystal structure of the basic region-leucine zipper (bZIP) domains of c-Fos and c-Jun bound to a DNA fragment containing the AP-1 binding site revealed that both domains form continuous α -helices, and the heterodimer grips the major groove of the DNA, similar to a pair of forceps.⁵

Natural products such as curcumin,⁶ dihydroguaiaretic acid,⁷ and an anthraquinone derivative⁸ were reported to inhibit the binding of AP-1 to the AP-1 binding site. However, three-dimensional (3D) structural information about the AP-1 binding of these inhibitors that is necessary for structure-based drug design is not well-known. In a previous report,⁹ we discovered a new cyclic disulfide decapeptide Ac-cyclo[Cys-Gly-Gln-Leu-Asp-Leu-Ala-Asp-Gly-Cys]-NH₂ (peptide **1**) that exhibits AP-1 inhibitory activity, using a de novo approach that exploited molecular modeling methods, such as molecular dynamics (MD) simulations, and docking studies based on the 3D structure of the bZIP domains derived from the X-ray structure.⁵ Furthermore, we built a 3D pharmacophore model based on the chemical and structural features of peptide **1**. These data were obtained from an alanine scan and structural studies involving a combination of MD simulation of the bZIP-peptide **1** complex

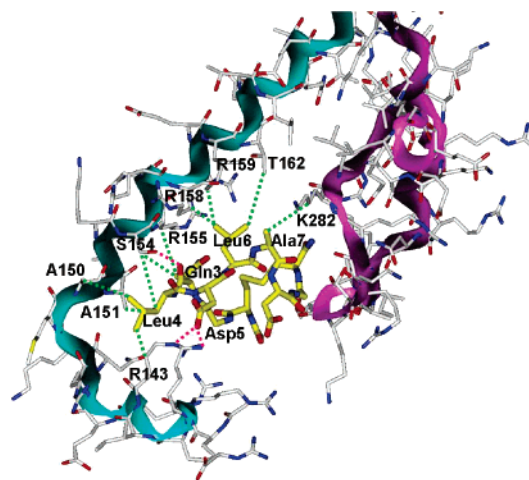


Figure 1. Binding model of peptide **1** (yellow) resulting from MD simulation. Ribbon representation of the basic domains (c-Fos, cyan; c-Jun, magenta). The residues of c-Fos and c-Jun that are involved in interactions are labeled with one-letter codes, and the residues of peptide **1** that are involved in interactions are labeled with three-letter codes. Red broken lines indicate putative hydrogen bonds and green broken lines indicate putative hydrophobic interactions. Hydrogen atoms are not shown for clarity.

with explicit water molecules (Figure 1) and NMR measurements of the peptide in water.⁹

Peptides generally have unfavorable properties for therapeutic drugs, such as poor bioavailability.¹⁰ Several approaches have been reported to convert bioactive peptides into nonpeptidic drug candidates known as peptidomimetics.^{10–12} In many cases, these peptidomimetics are peptide-like molecules, such as peptoids, and so further modifications are essential.

To avoid these problems, we designed nonpeptidic small molecules using a molecular modeling method based on a 3D pharmacophore model. This procedure could be described as “lead hopping” and has been employed as part of several recent *in silico* approaches.¹³ There are two general computational approaches, de novo design and 3D database searching, to identify new lead candidates with desired biological activity using a pharmacophore model.¹⁴ Although several successful

* To whom correspondence should be addressed. Phone: +81-76-431-8218. Fax: +81-76-431-8208. E-mail: keiichi_tsuchida@toyama-chemical.co.jp.

[†] Discovery Laboratories, Toyama Chemical Co., Ltd.

[‡] Research Laboratories, Toyama Chemical Co., Ltd.

[#] Kobe University School of Medicine.

[⊥] Kobe University Hospital.

[§] Kitasato University.

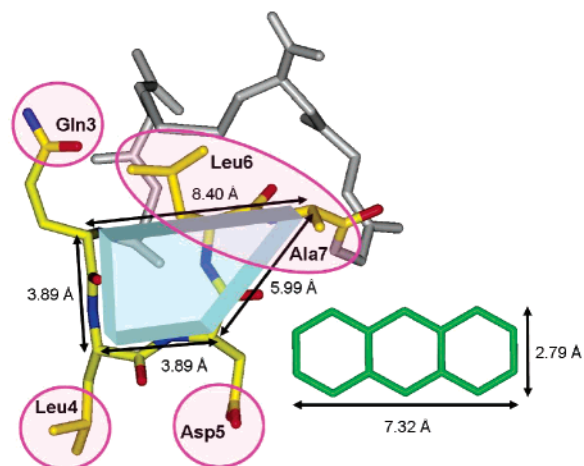


Figure 2. Pharmacophore model derived from peptide **1**. The pharmacophoric residues and the supplementary parts are colored yellow and gray, respectively. The pharmacophoric elements on peptide **1** are shown as circles and an ellipse in magenta. The main chain forms a trapezoid shape, the dimensions of which are shown by the arrows. An anthracene molecule of the same scale is depicted in green for a comparison of the sizes. Hydrogen atoms are not shown for clarity.

examples of these have been reported, the problems inherent in them have also been pointed out.^{15,16} In *de novo* design, output structures are particularly apt to be difficult to synthesize.^{15,16} In 3D database searching, novel structures cannot be obtained.¹⁵ Thus, we chose to search the compound library in our company to identify synthetically accessible scaffolds before general 3D database searching. We succeeded in finding several good scaffolds in the library. These scaffolds are synthetically accessible and easy to modify by our organic chemists. Through design efforts based on these scaffolds, we discovered new AP-1 inhibitors: 1-thia-4-azaspiro[4.5]decane and benzophenone derivatives.

In the current paper, we describe the design by a lead-hopping strategy and synthesis of nonpeptidic AP-1 inhibitors and their inhibitory activities as evaluated by AP-1 binding and cell-based reporter gene assays.

The Design of Nonpeptidic AP-1 Inhibitors. Lead-Hopping Strategy. Our pharmacophore model of AP-1 binding compounds is illustrated in Figure 2, which shows the 3D arrangement of the side-chain functional groups of the Gln-Leu-Asp-Leu-Ala residues in peptide **1**.⁹ A visual inspection revealed that the main chain of the five residues of peptide **1** has a β -turn-like conformation and a trapezoid shape (Figure 2). Its dimensions, which were measured as the distances between the α -carbons of Gln3-Leu4, Leu4-Asp5, Asp5-Ala7, and Gln3-Ala7, are 3.89, 3.89, 5.99, and 8.40 Å, respectively. Thus, we decided to design candidate small molecules for synthesis and evaluation by combining a suitably sized scaffold placed onto the trapezoid structure with the corresponding pharmacophoric elements, which constitute pivotal functional groups within the side chains of the five pharmacophoric residues of peptide **1**, to retain the 3D arrangement in the pharmacophore model.

Scaffold Design. In general, it is assumed that a scaffold should have a certain level of rigidity to maintain the correct spatial arrangement of each of the pharmacophoric elements. In addition, the substitution position to which a pharmacophoric element might be connected via a suitable linker should be flexible to ensure synthetic feasibility. In a different perspective, at least three substituents for each pharmacophoric element could be introduced that would allow sufficient pharmacophoric interactions. As depicted in Figure 2, the trapezoid was as large

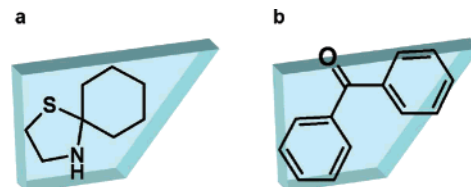


Figure 3. Fitting images of two scaffolds, 1-thia-4-azaspiro[4.5]decane (a) and benzophenone (b) to the trapezoid shown in Figure 2.

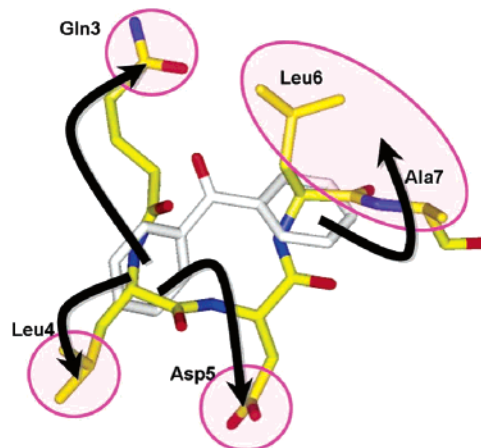


Figure 4. Illustration of the lead hopping of benzophenone. The superposition of the pharmacophoric residues of peptide **1** and the benzophenone scaffold is shown. The pharmacophoric elements on peptide **1** are shown as magenta-colored circles and an ellipse. The connections of the substituents from benzophenone are denoted by curved arrows.

as an anthracene molecule, which was therefore assumed to be the maximum size for a scaffold.

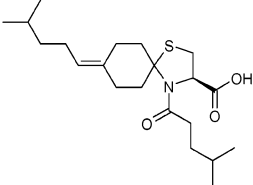
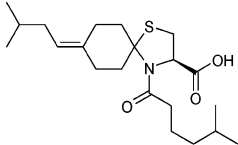
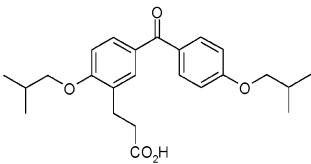
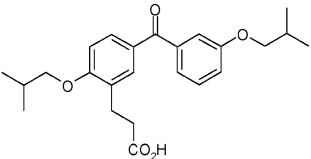
Although the main chain of the five pharmacophoric residues of peptide **1** had a planar trapezoid shape, the pharmacophoric elements were not located on the same plane. Thus, to maintain the pharmacophoric arrangement, it was desirable that the scaffold was not planar, but rather was twisted and compact, within limits.

On the basis of these considerations, by searching our compound library, we selected the two scaffolds that are depicted in Figure 3: 1-thia-4-azaspiro[4.5]decane and benzophenone (b) scaffolds.

Definition of Pharmacophoric Elements. Four pharmacophoric elements were defined from the five residues of the pharmacophore model: the carboxamide group of Gln3, the isobutyl group of Leu4, the carboxyl group of Asp5, and an isobutyl group that was adopted as a proxy for Leu6 and Ala7. The reason for using a proxy was that the two residues in question were adjacent to one another and could be regarded as one large hydrophobic element. Among these, the carboxyl group of Asp5 was regarded as a key pharmacophoric element, because substitution of the Asp5 had a significant effect in a previous alanine scan experiment;⁹ we therefore assumed that an acidic group at this position was essential for interactions with the basic regions of the bZIP domains. In addition, this carboxyl group appeared to be the only charged group and might have conferred desirable features in terms of drug design. We therefore produced various combinations of three or four pharmacophoric elements, while ensuring that a carboxyl group was incorporated into the newly designed molecules.

Scaffold Placement and Substitution Points. Only those atoms on a scaffold for which the introduction of a suitable substituent was synthetically feasible were viewed as potential

Table 1. Chemical Structure of Compounds 2–5 and Their Inhibitory Activities against AP-1

compd	structure	IC ₅₀ (μM)	
		binding assay ^a	luciferase assay ^b
1	Ac-c [Cys-Gly-Gln-Leu-Asp-Leu-Ala-Asp-Gly-Cys]-NH ₂	64	NT ^c
2		650	11.8
3		460	13.3
4		610	5.0
5		600	5.8

^a Inhibition of the binding of the AP-1 bZIP peptide to synthetic oligonucleotides containing the AP-1 binding site. ^b Inhibition of the expression of AP-1-luciferase by TPA-stimulated NIH3T3 cells. ^c NT: not tested.

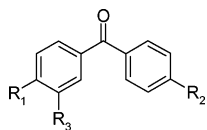
substitution points. Each scaffold was manually placed onto the trapezoid depicted in Figure 2 and interactively checked using a visual display. The position and orientation of the scaffolds were designed so that as many substitution points as possible were pointed in a favorable direction toward the corresponding pharmacophoric elements.

Combination of Scaffold and Pharmacophore Elements.

The candidate molecules for the synthesis were constructed by connecting the relevant pharmacophoric elements to suitable substitution points on each scaffold via linkers.

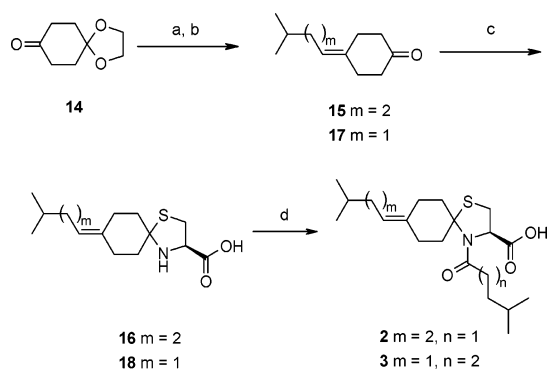
An example of substituent introduction featuring benzophenone is shown in Figure 4. The connections between the pharmacophoric elements at suitable substitution points are indicated by curved arrows. In this case, the pharmacophoric elements corresponding to Gln3, Leu4, and Asp5 could be connected by any atoms on the left-hand ring of the scaffold via linkers. Likewise, the centroid of Leu6 and Ala7 could be connected from any atom on the right-hand ring. The lengths and types of linkers used were carefully selected, taking synthetic feasibility into consideration.

Computational Evaluation of Designed Molecules. We examined the various possible combinations of substitution points, and the lengths and types of linkers, so that each pharmacophoric element was well suited to the pharmacophore model. Each of the designed molecules was computationally evaluated to verify the fact that the 3D pharmacophore requirements were met by a low-energy conformer. Conformational analyses were carried out to obtain low-energy conformers. All unique conformers that were within 6 kcal mol⁻¹ of the lowest energy were collected for each of the designed molecules. The selected low-energy conformers were then systematically superimposed onto peptide **1** using the least-squares fit¹⁷ of three or four of the pharmacophoric atoms: the δ-carbon atom of Gln3, the γ-carbon atoms of Leu4 and Asp5, and the centroid of the γ- and δ-carbon atoms of Leu6 and the β-carbon atom of Ala7. In addition, the overlapping volume between each conformer and the corresponding pharmacophoric residues in peptide **1**, and its ratio to the volume of the corresponding residues in peptide **1**, were calculated. Those compounds in which at least one conformer had a root-mean-square deviation

Table 2. Benzophenone Derivatives **4**, **6**–**13** and Their Inhibitory Activities in Binding Assay

compd	R ₁	R ₂	R ₃	% inhibition		IC ₅₀ (μM) ^c
				at 500 μM	at 1 mM	
4	O ^t Bu	O ^t Bu	CH ₂ CH ₂ CHO ₂ H	28	91	610
6	H	O ^t Bu	CH ₂ CH ₂ CHO ₂ H	10	14	>2000
7	O ^t Bu	H	CH ₂ CH ₂ CHO ₂ H	7	9	>2000
8	O ^t Bu	O ^t Bu	H	3	— ^b	ND ^c
9	O ⁿ Pr	O ^t Bu	CH ₂ CH ₂ CHO ₂ H	26	55	910
10	O ^t Bu	O ⁿ Pr	CH ₂ CH ₂ CHO ₂ H	25	42	930
11	OCH ₂ Ph	O ^t Bu	CH ₂ CH ₂ CHO ₂ H	51	97	420
12	O ^t Bu	OCH ₂ Ph	CH ₂ CH ₂ CHO ₂ H	45	— ^b	ND ^c
13	O ^t Bu	O ^t Bu	CH ₂ CH ₂ CONH ₂	5	— ^b	ND ^c

^a 50% inhibition concentration was determined from the concentration–response curve (125–2000 μM). ^b % inhibition was not determined at this concentration due to precipitation. ^c ND: not determined.

Scheme 1^a

^a Reagents: (a) Me₂CHCH₂CH₂CH₂PPh₃Br (for **15**) or Me₂CHCH₂CH₂-PPh₃I (for **17**), *n*-butyllithium, THF; (b) 6 M HCl, 1,4-dioxane; (c) L-cysteine, aq EtOH; (d) 4-methylpentanoic acid (for **2**) or 5-methylhexanoic acid (for **3**), oxalyl chloride, Et₃N, CH₂Cl₂.

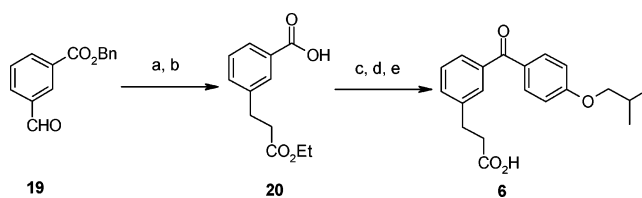
(RMSD) value ≤ 1.0 Å under a three- or four-point superposition with the corresponding residues of peptide **1**, and an overlapping volume ratio ≥ 0.5, were selected as small-molecule inhibitor candidates for synthesis and biological evaluation.

Biological Evaluation of the Compounds Synthesized. The AP-1 inhibitory activities of the compounds synthesized were evaluated using enzyme-linked immunosorbent assay (ELISA)-based AP-1 DNA-binding and cell-based reporter assays (Table 1; compounds **2**–**5**).

Furthermore, the synthesis of benzophenone derivatives and the evaluation of their inhibitory activities were performed to verify our pharmacophore model (Table 2; compounds **6**–**13**).

Chemistry

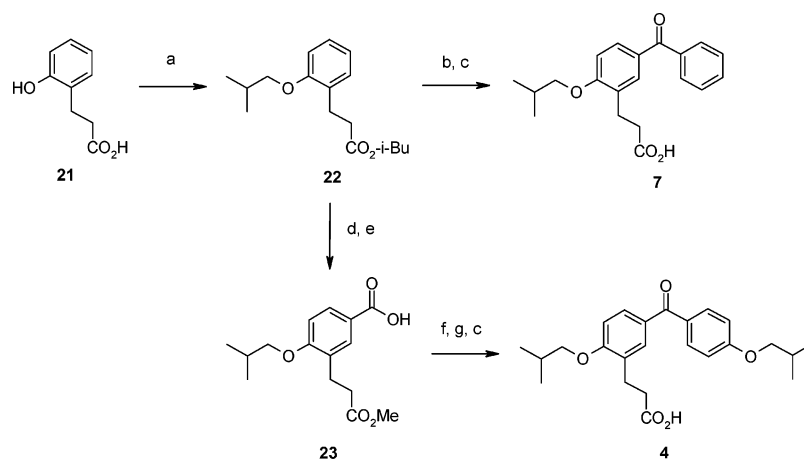
Synthesis of the (*R*)-4-(4-methylpentanoyl)-1-thia-4-azaspiro[4.5]decane compound **2** was carried out as outlined in Scheme 1. The starting material, 1,4-cyclohexanedione monoethylene ketal (**14**), was subjected to the Wittig reaction with 4-methylpentyltriphenylphosphonium bromide and *n*-butyllithium to afford 4-(4-methylpentylidene)cyclohexanone (**15**) after an acid-catalyzed deprotection procedure. Treatment of **15** with L-cysteine in aqueous EtOH produced the spiro[cyclohexane-1,2'-thiazolidine] compound **16**, which was treated with 4-methylpentanoyl chloride in the presence of Et₃N to provide the target molecule **2**.¹⁸ The structurally analogous spiro compound **3**, 1-thia-4-azaspiro[4.5]decane-3-carboxylic acid, 8-(3-methylbutylidene)-4-(5-methylhexanoyl), was prepared by the same procedure.

Scheme 2^a

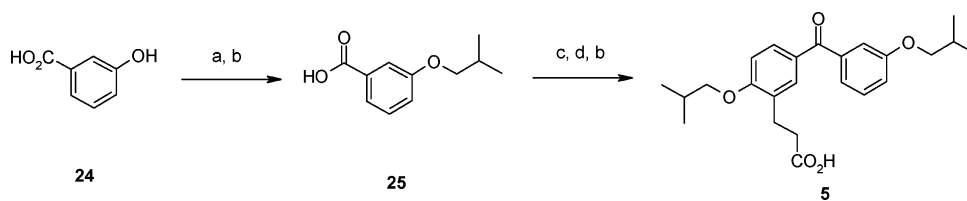
^a Reagents: (a) (EtO)₂P(O)CH₂CO₂Et, NaH, DMF; (b) H₂, Pd–C, EtOH; (c) oxalyl chloride, DMF, CH₂Cl₂; (d) isobutoxybenzene, AlCl₃, CH₂Cl₂; (e) NaOH–H₂O, EtOH.

Syntheses of mono- and di-isobutoxy derivatives of 3-(3-benzoylphenyl)propionic acid (**4**–**7**) were carried out as illustrated in Schemes 2–4. 3-[3-(4-Isobutoxybenzoyl)phenyl]propionic acid (**6**) was prepared via the Horner–Emmons reaction of benzyl 3-formylbenzoate (**19**) with ethyl diethylphosphonoacetate and NaH, which was followed by Pd–C-catalyzed hydrogenation to yield 3-(ethoxycarbonyl)benzoic acid (**20**). The corresponding acid chloride generated by treatment with oxalyl chloride was allowed to react with isobutoxybenzene¹⁹ in the presence of AlCl₃ in CH₂Cl₂ to give an ethyl ester, which on alkaline ester hydrolysis provided compound **6** (Scheme 2). Compound **7** (Scheme 3), which is a regioisomer of the isobutoxy group of **6**, was prepared via isobutyl 3-(2-isobutoxyphenyl)propionate (**22**), which was subjected to a regioselective Friedel–Crafts benzylation. Compound **22** was also employed for the synthesis of 3-[2-isobutoxy-5-(4-isobutoxybenzoyl)phenyl]propionic acid (**4**). The regioselective formylation reaction²⁰ of **22** followed by NaClO₂–H₂O₂ oxidation²¹ afforded the monocarboxylic acid **23**, and coupling its acyl chloride with isobutoxybenzene afforded compound **4**. The regioisomer **5**, 3-[2-isobutoxy-5-(3-isobutoxybenzoyl)phenyl]propionic acid, was prepared via coupling of **22** with the acyl chloride of 3-isobutoxybenzoic acid (**25**) in the presence of AlCl₃ (Scheme 4).

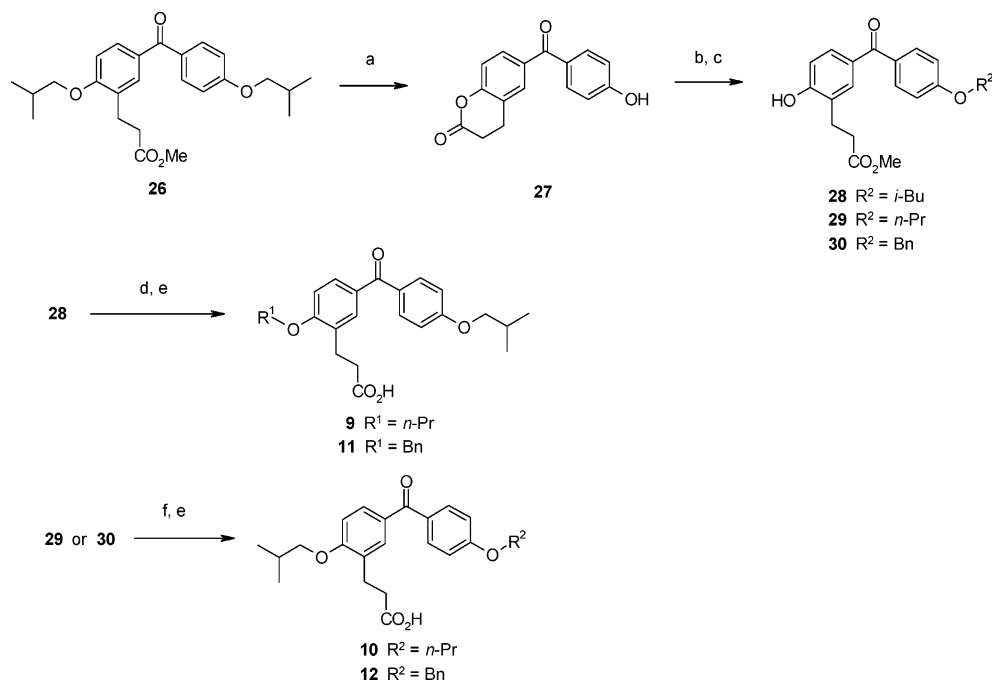
Exchange of either one of the two isobutoxy groups in **4** with a propoxy or benzyloxy ether moiety was also considered as outlined in Scheme 5. The methyl ester of **4** (compound **26**) was subjected to AlCl₃-catalyzed lactonization accompanied by cleavage of the isobutoxy linkage to produce 6-(4-hydroxybenzoyl)-3,4-dihydrocoumarin (**27**). The liberated phenolic hydroxyl group was then subjected to the Mitsunobu reaction with R²-OH (2-methylpropanol, propanol, or benzyl alcohol) in the presence of diisopropyl azodicarboxylate (DIAD) and triphenylphosphine in tetrahydrofuran (THF) followed by MeONa-

Scheme 3^a

^a Reagents: (a) isobutyl bromide, K₂CO₃, DMF; (b) benzoyl chloride, AlCl₃, CH₂Cl₂; (c) NaOH–H₂O, acetone (for **4**) or EtOH (for **7**); (d) Cl₂CHOMe, AlCl₃, CH₂Cl₂, then MeOH, Δ; (e) NaClO₂, H₂O₂, NaH₂PO₄, *aq.* MeCN; (f) oxalyl chloride, DMF, CH₂Cl₂; (g) isobutoxybenzene, AlCl₃, CH₂Cl₂.

Scheme 4^a

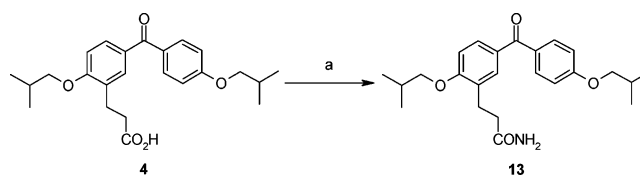
^a Reagents: (a) isobutyl bromide, K₂CO₃, DMF; (b) NaOH–H₂O, acetone; (c) oxalyl chloride, DMF, CH₂Cl₂; (d) compound **22**, AlCl₃, CH₂Cl₂.

Scheme 5^a

^a Reagents: (a) AlCl₃, 1,2-dichloroethane; (b) R²-OH, DIAD, Ph₃P, THF; (c) MeONa–MeOH, THF; (d) R¹-Br, K₂CO₃, DMF; (e) NaOH–H₂O, acetone; (f) isobutyl bromide, K₂CO₃, DMF.

catalyzed methanolysis to yield the corresponding alkyl ethers **28–30**. Compound **28** was alkylated with R¹-Br (propyl bromide or benzyl bromide), followed by hydrolysis with alkali to yield **9** and **11** as depicted in Scheme 5. The regioisomeric analogues **10** and **12** were prepared similarly via **29** (R² = propyl) and **30** (R² = benzyl), respectively.

Synthesis of carboxamide of **4** (compound **13**) was carried out as outlined in Scheme 6. Compound **4** was treated with oxalyl chloride and catalytic DMF leading to the acid chloride,

Scheme 6^a

^a Reagents: (a) oxalyl chloride, DMF, THF, then NH₄OH.

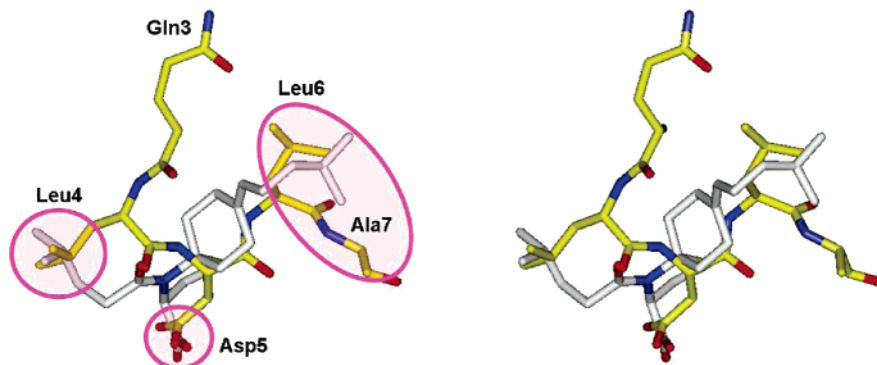


Figure 5. Stereoview of the superposition of Leu-Asp-Leu-Ala of peptide **1** (yellow) with compound **2** (white). The fitted points are shown as magenta-colored circles and an ellipse. Hydrogen atoms are not shown for clarity.

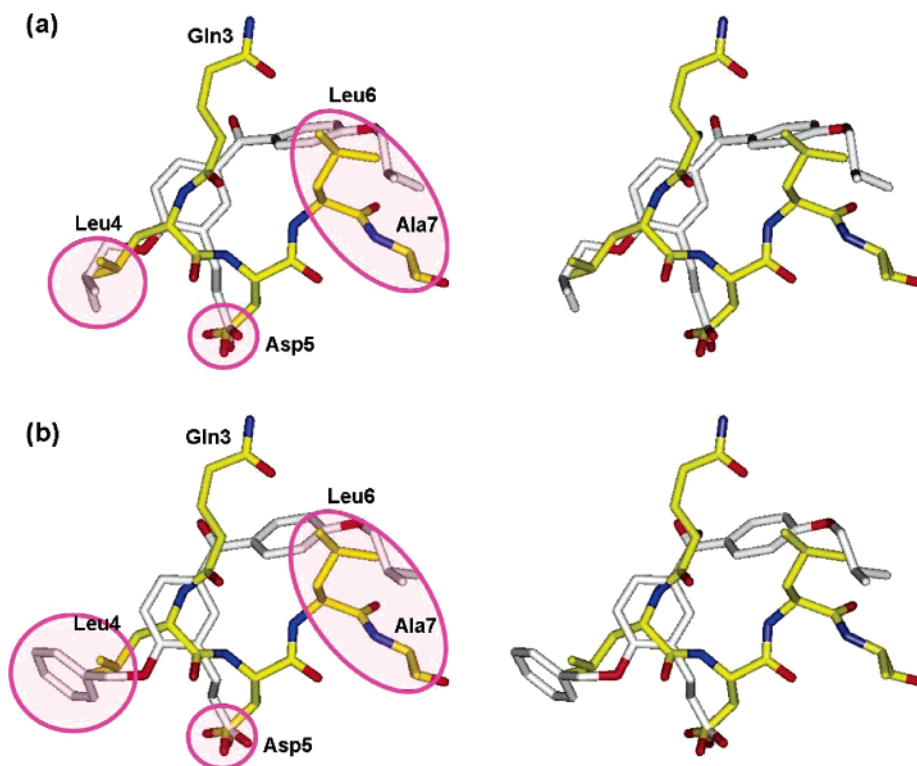


Figure 6. Stereoviews of the superposition of Leu-Asp-Leu-Ala of peptide **1** (yellow) with (a) compound **4** (white) and (b) compound **11** (white). The fitted points are shown as magenta-colored circles and an ellipse. Hydrogen atoms are not shown for clarity.

which was converted to propionamide **13** with ammonium hydroxide. Bis(4-isobutoxyphenyl)methanone (**8**) was prepared from commercially purchased bis(4-hydroxyphenyl)methanone by O-isobutylation with isobutyl bromide and K_2CO_3 in DMF.

Results and Discussion

Evaluation of Designed Compounds. The designed compounds were synthesized and evaluated using an ELISA-based AP-1 DNA-binding assay. Among these, compounds **2** and **3** bearing 1-thia-4-azaspiro[4.5]decane as a scaffold, and compounds **4** and **5**, bearing benzophenone as a scaffold, inhibited the binding of AP-1 bZIP and oligonucleotides containing the AP-1 binding site (Table 1; $IC_{50} = 460\text{--}650\ \mu\text{M}$). The three pharmacophoric elements of these compounds corresponded to Leu4, Asp5, and the centroid of Leu6 and Ala7 of peptide **1**. As examples, the best-fit superpositions of compounds **2** and **4** onto peptide **1** based on the pharmacophore model are shown in Figures 5 and 6a, respectively. The three pairs of pharmacophoric points that were used for overlapping are shown as circles and an ellipse in these figures. The three overlapped

points within compound **2** were the carbon atom of the carboxyl group plus the carbon atoms at the branched positions of the 4-methylpentanoyl and 4-methylpentylidene groups. The RMSD value resulting from the superposition of the three pharmacophoric points was $0.89\ \text{\AA}$, and the energy of this best-fitted conformer relative to the lowest energy was $2.01\ \text{kcal mol}^{-1}$. The three overlapped points within compound **4** were the carbon atom of the carboxyl group plus the carbon atoms at the branched positions of the isobutyl groups. The RMSD value resulting from the superposition of the three pharmacophoric points was $0.92\ \text{\AA}$, and the energy of this best-fitted conformer relative to the lowest energy was $2.46\ \text{kcal mol}^{-1}$. The structural isomers **2** and **3**, in which the lengths of methylene linkers between the 1-thia-4-azaspiro[4.5]decane scaffold and each isobutyl pharmacophore element were different, showed similar activity. The RMSD value obtained by the best-fit superposition of compound **3** and peptide **1** was $0.64\ \text{\AA}$, and the energy of the best-fitted conformer relative to the lowest energy was $1.73\ \text{kcal mol}^{-1}$; thus the 3D pharmacophore requirement was met by compound **3**, as well as compound **2**. Because compounds

4 and **5**, in which only the substitution position of an isobutoxy moiety corresponding to the centroid of Leu6 and Ala7 differed, showed similar activity, there might be some allowance in the hydrophobic region of the pharmacophore. This was consistent with our assumption that Leu6 and Ala7 comprised one large hydrophobic element. These small-molecule compounds showed lower inhibitory activity than peptide **1** ($IC_{50} = 64 \mu M$). The results would be acceptable, given that these compounds have only three pharmacophore elements compared to the cyclic decapeptide.

Subsequently, we evaluated the effects of these compounds on the transactivation activity of AP-1 using a cell-based AP-1 reporter gene assay (Table 1). Compounds **2–5** showed dose-dependent inhibitory activities in this assay, similar to AP-1 DNA-binding inhibition. Thus, taking into account both the inhibitory activities and synthetic feasibility, we carried out further structural development of the benzophenone derivatives.

Conversion of Substituents on Benzophenone Derivatives. To verify the pharmacophoric elements, we designed and synthesized several derivatives based on compound **4**, and evaluated their inhibitory activities on AP-1 DNA-binding (Table 2).

The conversion of each substituent of compound **4** to hydrogen (compounds **6–8**) resulted in a considerable loss of inhibitory activity in the binding assay; thus, the importance of the three pharmacophore elements was confirmed.

In addition, the conversion of each isobutoxy group to an *n*-propoxy group (compounds **9** and **10**) resulted in a moderate loss of inhibitory activity at 1 mM. This finding may suggest a requirement for bulkiness of the branched chain alkyl groups.

Furthermore, compounds **11** and **12**, in which each isobutoxy group was substituted with a benzyloxy group, showed similar inhibitory activities to compound **4**, which implied that both aliphatic and aromatic substituents were acceptable hydrophobic elements at this position. The best-fit superposition of compound **11** and peptide **1** is shown in Figure 6b. The three overlapped points within compound **11** are the carbon atom of the carboxyl group, the carbon atom at the branched position of the isobutyl group, and the carbon atom at the root of the benzene ring in the benzyl group. The RMSD value obtained by the superposition of the three pharmacophoric points was 0.93 Å, and the energy of this best-fitted conformer relative to the lowest energy was 4.58 kcal mol⁻¹. The conformation and orientation of compound **11** were similar to those of compound **4** (Figure 6).

Finally, we converted the R₃ substituent to investigate the importance of the carboxyl group. The conversion into carbonyl (compound **13**) resulted in a considerable loss of inhibitory activity. This result clearly demonstrates the significance of the ionic interactions. This appears to support our initial hypothesis that the basic lysine and/or arginine in the basic region of bZIP domains might take part in the interactions with peptide **1**.

The above-mentioned results demonstrate that the optimal arrangement of at least three pharmacophoric elements is fundamental. In addition, we suggest that it might be possible to enhance the inhibitory activity by the further introduction of a fourth pharmacophoric element corresponding to Gln3 of peptide **1** that showed more potent inhibitory activity.

Conclusions

We converted cyclic peptide **1** to small-molecule AP-1 inhibitors using a lead-hopping approach based on a 3D pharmacophore model that was derived from the peptide. New AP-1 inhibitors, 1-thia-4-azaspiro[4.5]decane and benzophenone

derivatives, were discovered using this combination of computational methods and medicinal chemistry intuition. Our study demonstrated the reliability of the 3D pharmacophore model and its utility in the discovery of AP-1 inhibitors. Additionally, the possibility of further improvement of the benzophenone derivatives was suggested by the results of the conversion of the substituents. The benzophenone derivatives were considered to be an attractive lead series, because they exhibited AP-1 inhibitory activities not only in the binding assay but also in the cell-based assay. The continuous optimization of this series might produce drugs that can be used against AP-1 for the treatment of various diseases.

Experimental Section

Molecular Modeling. All molecular modeling was performed using the SYBYL software package version 6.5²² running on a Silicon Graphics Power Indigo2 workstation. All of the compounds designed for use in this study were built using the SKETCH module. The carboxyl group of the designed compounds was deprotonated to imitate physiological conditions. The designed compounds were minimized using the Powell method in the MAXIMIN2 module of SYBYL to reach a final convergence of 0.01 kcal mol⁻¹ Å⁻¹; the MMFF94 force field and the MMFF94 charges²³ were employed for the energy minimizations. Electrostatic interactions were taken into consideration using a distance-based dielectric constant of 78.3 to simulate an aqueous environment.

Conformational analysis of each of the designed compounds was carried out using the Random Search module implemented in SYBYL. An absolute energy cutoff of 300 kcal mol⁻¹ was used to remove high energy conformations. The energy values during the optimization were computed with the MMFF94 force field and the MMFF94 charges. The number of maximum cycles was set to 1000. Within each cycle, the bonds that were defined as rotatable were set to random torsion angles and the compounds were then minimized. The number of maximum hits was set to 6. Unique conformers were distinguished by setting a RMS threshold of 0.2 Å, with chirality checking if necessary. The systematical superposition of collected low-energy conformers was carried out using the FIT routine in SYBYL.

The overlapping volume and the volume of the corresponding residues in peptide **1** as a template were calculated using the MVOLUME and VOLUME routines in SYBYL, respectively.

Chemistry. Melting points were determined using a B-545 melting point apparatus (Büchi Lab., Flawil, Switzerland) and were uncorrected. Proton NMR (¹H NMR) spectra were recorded on a JEOL JNM-AL 400 spectrometer (JEOL Ltd., Tokyo, Japan) using tetramethylsilane as the internal standard. Chemical shifts are reported in ppm (δ units), and the signal patterns are designated as s (singlet), d (doublet), t (triplet), q (quartet), m (multiplet), and br (broad). Column chromatography was carried out using PSQ100B silica gel of 75–200 μm (Fuji Silysia Chemical, Aichi, Japan). Low-resolution mass spectra (MS) were obtained on a Hitachi M-8000 mass spectrometer system equipped with an electrospray ionization interface (Hitachi Ltd., Tokyo, Japan). Elemental analysis (C, H, and N) was performed at Toyama Industrial Technology Center (Toyama, Japan), and all results were within $\pm 0.4\%$ of the theoretical values. Unless otherwise noted, all solvents, chemicals, and reagents were obtained commercially and used without purification. Peptide **1** has been previously described.⁹

4-(4-Methylpentylidene)cyclohexanone (15). To a stirred and cooled ($-45 \text{ }^\circ\text{C}$) suspension of 4-methylpentyltriphenylphosphonium bromide (13.1 g, 30.7 mmol) in THF (40 mL) was added dropwise *n*-butyllithium (1.6 M in hexane, 19.2 mL, 30.7 mmol). The mixture was then warmed to 0 $^\circ\text{C}$ over 20 min. A solution of 1,4-cyclohexanedione monoethylene ketal (**14**) (4.00 g, 25.6 mmol) in THF (20 mL) was added dropwise to the resulting phosphorane solution at 0–5 $^\circ\text{C}$. Subsequently, the reaction mixture was allowed to warm to room temperature and was stirred for 1 h. The mixture was quenched with water (100 mL) and extracted with EtOAc (1

× 100 mL). The aqueous layer was extracted with EtOAc (1 × 50 mL). The combined organic extracts were washed with water (1 × 100 mL) and brine (1 × 100 mL), dried over MgSO₄, and concentrated under reduced pressure. The residue was purified by chromatography (silica gel 150 g, 5:1 hexane/EtOAc) to give 8-(4-methylpentylidene)-1,4-dioxaspiro[4.5]decane (5.40 g, 94%) as a colorless oil: ¹H NMR (400 MHz, CDCl₃) δ 0.87 (6H, d, *J* = 6.6 Hz), 1.21 (2H, q, *J* = 7.5 Hz), 1.46–1.62 (1H, m), 1.62–1.72 (4H, m), 1.99 (2H, q, *J* = 7.5 Hz), 2.21 (2H, t, *J* = 6.3 Hz), 2.27 (2H, t, *J* = 6.5 Hz), 3.97 (4H, s), 5.13 (1H, t, *J* = 7.5 Hz).

A mixture of the ketal (1.00 g, 4.46 mmol) obtained above and 6 M HCl (5 mL) in 1,4-dioxane (10 mL) was stirred at room temperature for 9 h before dilution with CHCl₃ (50 mL) and water (30 mL). The aqueous layer separated was extracted with CHCl₃ (1 × 30 mL), and the combined organic extracts were washed with water (1 × 30 mL) and brine (1 × 30 mL), dried over MgSO₄, and concentrated under reduced pressure. The residue was purified by chromatography (silica gel 100 g, 10:1 hexane/EtOAc) to give **15** (0.77 g, 96%) as a colorless oil: ¹H NMR (400 MHz, CDCl₃) δ 0.90 (6H, d, *J* = 6.6 Hz), 1.16–1.32 (2H, m), 1.48–1.66 (1H, m), 2.04 (2H, q, *J* = 7.6 Hz), 2.36–2.56 (8H, m), 5.30–5.38 (1H, m).

4-(3-Methylbutylidene)cyclohexanone (17). Compound **14** was treated by the procedure described for **15** except using 3-methylbutyltriphenylphosphonium iodide to afford **17** (65%) as a colorless oil: ¹H NMR (400 MHz, CDCl₃) δ 0.91 (6H, d, *J* = 6.6 Hz), 1.56–1.72 (1H, m), 1.90–1.97 (2H, m), 2.36–2.54 (8H, m), 5.37 (1H, t, *J* = 7.3 Hz); MS *m/z* 167 (M + H)⁺.

(R)-8-(4-Methylpentylidene)-1-thia-4-azaspiro[4.5]decane-3-carboxylic Acid (16). A mixture of **15** (1.20 g, 6.66 mmol) and L-cysteine (1.21 g, 9.99 mmol) in a mixture of 7:3 EtOH/water (36 mL) was stirred at room temperature for 3 h and at 40 °C for 5 h. The reaction mixture was evaporated under reduced pressure before dilution with water (100 mL). The product precipitated was collected by filtration and washed with water (3 × 30 mL) and hexane (3 × 30 mL) to afford **16** (1.18 g, 63%) as a light brown solid: ¹H NMR (400 MHz, CDCl₃) δ 0.88 (6H, d, *J* = 6.6 Hz), 1.20 (2H, q, *J* = 7.3 Hz), 1.46–1.60 (1H, m), 1.84–2.64 (10H, m), 3.22–3.34 (1H, m), 3.36–3.50 (1H, m), 4.33 (1H, t, *J* = 7.2 Hz), 5.10–5.22 (1H, m), 5.30–5.70 (2H, br); MS *m/z* 284 (M + H)⁺, 282 (M - H)⁻.

(R)-8-(3-Methylbutylidene)-1-thia-4-azaspiro[4.5]decane-3-carboxylic Acid (18). Compound **17** (5.00 g, 30.1 mmol) was treated by the procedure described for **16** to afford **18** (4.40 g, 54%) as a white solid: ¹H NMR (400 MHz, CDCl₃) δ 0.87 (6H, d, *J* = 6.3 Hz), 1.50–1.64 (1H, m), 1.82–2.14 (6H, m), 2.16–2.64 (4H, m), 3.22–3.32 (1H, m), 3.42 (1H, dd, *J* = 11.3, 7.4 Hz), 3.78 (2H, br s), 4.32 (1H, t, *J* = 7.4 Hz), 5.19 (1H, t, *J* = 7.3 Hz); MS *m/z* 268 (M - H)⁻.

(R)-4-(4-Methylpentanoyl)-8-(4-methylpentylidene)-1-thia-4-azaspiro[4.5]decane-3-carboxylic Acid (2). To a stirred solution of 4-methylpentanoic acid (225 mg, 1.94 mmol) in CH₂Cl₂ (5 mL) at room temperature was added dropwise oxalyl chloride (246 mg, 1.94 mmol) followed by the addition of DMF (50 μL), and the mixture was stirred at the same temperature for 2 h. The mixture was cooled in an ice bath before the sequential addition of **16** (500 mg, 1.76 mmol) and Et₃N (535 mg, 5.29 mmol), and then the mixture was stirred at room temperature for 2 h. The resulting mixture was treated with CHCl₃ (30 mL) and water (30 mL), followed by acidification to pH 2 with 6 M HCl, and the layers were separated. The aqueous layer was extracted with CHCl₃ (30 mL), and the combined organic extracts were washed with water (1 × 30 mL) and brine (1 × 30 mL), dried over MgSO₄, and concentrated under reduced pressure. The residue was purified by chromatography (silica gel 50 g, 10:1 CHCl₃/MeOH) to give **2** (380 mg, 56%) as a white solid, which was crystallized from CH₂Cl₂/hexane to give colorless crystals, mp 144–145 °C: ¹H NMR (400 MHz, CDCl₃) δ 0.87 (6H, d, *J* = 6.6 Hz), 0.88 (6H, d, *J* = 5.6 Hz), 1.20 (2H, q, *J* = 7.0 Hz), 1.34–1.78 (5H, m), 1.86–2.72 (9H, m), 2.84–3.38 (4H, m), 4.90–5.02 (1H, m), 5.06–5.16 (1H, m), 5.25–5.45 (1H, br); MS *m/z* 381 (M - H)⁻. Anal. (C₂₁H₃₅NO₃S) C, H, N.

(R)-8-(3-Methylbutylidene)-4-(5-methylhexanoyl)-1-thia-4-azaspiro[4.5]decane-3-carboxylic Acid (3). Compound **18** (500 mg, 1.86 mmol) was treated by the procedure described for **2** except using 5-methylhexanoic acid to afford **3** (305 mg, 43%) as a white solid, which was crystallized from CH₂Cl₂/hexane to give colorless crystals, mp 135–138 °C: ¹H NMR (400 MHz, CDCl₃) δ 0.87 (12H, d, *J* = 6.8 Hz), 1.10–1.24 (2H, m), 1.48–1.74 (5H, m), 1.76–2.50 (7H, m), 2.56–2.72 (1H, m), 2.84–3.34 (5H, m), 4.90–5.00 (1H, m), 5.10–5.20 (1H, m); MS *m/z* 382 (M + H)⁺, 380 (M - H)⁻. Anal. (C₂₁H₃₅NO₃S) C, H, N.

3-(2-Ethoxycarbonylethyl)benzoic Acid (20). To a stirred suspension of NaH (60% dispersion in mineral oil, 1.37 g, 34.3 mmol) in DMF (75 mL) at 10–15 °C was added dropwise ethyl diethylphosphonoacetate (7.69 g, 34.3 mmol). The mixture was then stirred at room temperature for 30 min. To the stirred and ice-cooled mixture was added dropwise benzyl 3-formylbenzoate (**19**) (7.50 g, 31.2 mmol) before being stirred at room temperature for 30 min. The reaction mixture was poured into a mixture of EtOAc (100 mL) and 1 M HCl (50 mL), and the aqueous layer separated was extracted with EtOAc (1 × 50 mL). The organic extracts were washed with water (1 × 100 mL) and brine (1 × 100 mL), dried over MgSO₄, and concentrated under reduced pressure. The residue was purified by chromatography (silica gel 100 g, 3:1 hexane/EtOAc) to give benzyl 3-((*E*)-2-ethoxycarbonylvinyl)benzoate (9.12 g, 94%) as a colorless oil: ¹H NMR (400 MHz, CDCl₃) δ 1.34 (3H, t, *J* = 7.1 Hz), 4.27 (2H, q, *J* = 7.1 Hz), 5.38 (2H, s), 6.50 (1H, d, *J* = 16.0 Hz), 7.31–7.56 (6H, m), 7.70 (1H, d, *J* = 8.1 Hz), 7.70 (1H, d, *J* = 16.0 Hz), 8.08 (1H, d, *J* = 7.8 Hz), 8.22 (1H, s); MS *m/z* 311 (M + H)⁺.

A suspension of the α,β-unsaturated ester (8.50 g, 274 mmol) obtained above in EtOH (85 mL) was stirred at 40 °C under the atmospheric pressure of H₂ in the presence of 10% Pd-C (1.70 g). The mixture was filtered through Celite after 3 h, and the residue was washed with EtOH (3 × 20 mL). The filtrate was concentrated under reduced pressure to afford the semisolid residue, which was triturated with hexane (100 mL) to give **20** (5.87 g, 96%) as an off-white solid: ¹H NMR (400 MHz, CDCl₃) δ 1.24 (3H, t, *J* = 7.2 Hz), 2.67 (2H, t, *J* = 7.7 Hz), 3.03 (2H, t, *J* = 7.7 Hz), 4.14 (2H, q, *J* = 7.2 Hz), 7.41 (1H, t, *J* = 7.7 Hz), 7.47 (1H, d, *J* = 7.7 Hz), 7.92–8.03 (2H, m); MS *m/z* 221 (M - H)⁻.

Isobutyl 3-(2-Isobutoxyphenyl)propionate (22). A mixture of 3-(2-hydroxyphenyl)propionic acid (**21**) (10.0 g, 60.2 mmol), K₂CO₃ (41.6 g, 301 mmol), and isobutyl bromide (33.0 g, 241 mmol) in DMF (100 mL) was heated with vigorous stirring at 140 °C for 1 h. After cooling to room temperature, the reaction mixture was treated with EtOAc (150 mL) and water (300 mL) followed by acidification to pH 4 with 6 M HCl. The organic extract was washed with water (1 × 50 mL) and brine (1 × 50 mL), dried over MgSO₄, and concentrated under reduced pressure. The residue was purified by chromatography (silica gel 300 g, 5:1 hexane/EtOAc) to give **22** (15.4 g, 92%) as a colorless oil: ¹H NMR (400 MHz, CDCl₃) δ 0.91 (6H, d, *J* = 7.1 Hz), 1.05 (6H, d, *J* = 7.1 Hz), 1.84–1.96 (1H, m), 2.06–2.18 (1H, m), 2.63 (2H, t, *J* = 7.9 Hz), 2.97 (2H, t, *J* = 7.9 Hz), 3.74 (2H, d, *J* = 6.4 Hz), 3.85 (2H, d, *J* = 6.6 Hz), 6.78–6.88 (2H, m), 7.12–7.20 (2H, m); MS *m/z* 279 (M + H)⁺.

4-Isobutoxy-3-(2-methoxycarbonylethyl)benzoic Acid (23). To a stirred solution of **22** (10.0 g, 35.9 mmol) in CH₂Cl₂ (50 mL) at -30 °C were successively added AlCl₃ (9.58 g, 71.8 mmol) and dichloromethyl methyl ether (4.96 g, 43.1 mmol), and the mixture was stirred at -10 °C for 1 h. After addition of MeOH (50 mL), the resulting mixture was stirred under reflux for 2 h before cooling to room temperature. The reaction mixture was poured into ice-water (200 mL), and the organic layer was sequentially washed with 1 M HCl (1 × 50 mL) and water (1 × 50 mL), and concentrated under reduced pressure to give aldehyde as a brown oil, which was used without further purification. The aldehyde thus obtained was dissolved in CH₃CN (20 mL). To the stirred solution were added a solution of NaH₂PO₄·2H₂O (15.1 g, 96.8 mmol) in water (20 mL) and 30% aqueous H₂O₂ (6.11 g, 53.9 mmol) in sequence. A solution of NaClO₂ (80% purity, 6.50 g, 57.5 mmol) in water (10 mL) was added dropwise over 10 min to the ice-cooled

mixture with stirring before being stirred at room temperature for 1 h. The solid material that had precipitated during the reaction was filtered and washed with water (2×20 mL) to give **23** (7.32 g, 73%) as a pale yellow solid: $^1\text{H NMR}$ (400 MHz, CDCl_3) δ 1.06 (6H, d, $J = 6.6$ Hz), 2.08–2.22 (1H, m), 2.64 (2H, t, $J = 7.8$ Hz), 3.00 (2H, t, $J = 7.8$ Hz), 3.69 (3H, s), 3.82 (2H, d, $J = 6.6$ Hz), 6.86 (1H, d, $J = 8.7$ Hz), 7.91 (1H, d, $J = 2.2$ Hz), 7.98 (1H, dd, $J = 8.7, 2.2$ Hz); MS m/z 279 ($\text{M} - \text{H}$) $^-$.

3-Isobutoxybenzoic Acid (25). A mixture of 3-hydroxybenzoic acid (**24**) (10.0 g, 72.4 mmol), K_2CO_3 (25.0 g, 181 mmol), and isobutyl bromide (29.8 g, 217 mmol) in DMF (100 mL) was heated with stirring at 120 °C for 2 h. The reaction mixture was then cooled to room temperature, treated with water (300 mL) followed by acidification to pH 4 with 6 M HCl, and extracted with EtOAc (100 mL). The organic layer was washed with water (1×100 mL) and brine (1×100 mL), dried over MgSO_4 , and evaporated under reduced pressure to afford di-O-isobutylated product as a pale yellow oil. The di-O-isobutylated product thus obtained was dissolved in acetone (100 mL), and then 20 wt % aqueous NaOH (50.0 g) was added to the mixture at room temperature. The reaction mixture was allowed to cool to room temperature after being stirred at 50 °C for 2 h, and then water (300 mL) was added. The mixture was acidified to pH 1 with 12 M HCl and stirred at room temperature for 30 min, and the resulting precipitate was collected by filtration and washed with water (2×50 mL) to give **25** (9.85 g, 70%) as a white solid: $^1\text{H NMR}$ (400 MHz, CDCl_3) δ 1.05 (6H, d, $J = 6.4$ Hz), 2.04–2.18 (1H, m), 3.78 (2H, d, $J = 6.6$ Hz), 7.16 (1H, ddd, $J = 7.9, 2.6, 0.5$ Hz), 7.37 (1H, t, $J = 7.9$ Hz), 7.62 (1H, dd, $J = 2.6, 1.6$ Hz), 7.70 (1H, d, $J = 7.9$ Hz); MS m/z 193 ($\text{M} - \text{H}$) $^-$.

3-[2-Isobutoxy-5-(4-isobutoxybenzoyl)phenyl]propionic Acid (4). To a stirred solution of **23** (2.00 g, 7.13 mmol) and DMF (0.1 mL) in CH_2Cl_2 (20 mL) at room temperature was added oxalyl chloride (1.09 g, 8.59 mmol). After continuous stirring for 1 h, the mixture was cooled with ice–water before the sequential addition of AlCl_3 (2.09 g, 15.7 mmol) and isobutoxybenzene (1.29 g, 8.59 mmol). After being stirred at 5–10 °C for 30 min, the reaction mixture was poured into a mixture of ice (20 g) and 6 M HCl (30 mL). The layers were separated, and the organic layer was washed with water (1×20 mL) and brine (1×20 mL), dried over MgSO_4 , and concentrated under reduced pressure. The residue was purified by chromatography (silica gel 50 g, 5:1 hexane/EtOAc) to give methyl 3-[2-isobutoxy-5-(4-isobutoxybenzoyl)phenyl]propionate (**26**) (2.36 g, 80%) as a white crystalline solid, mp 78–79 °C: $^1\text{H NMR}$ (400 MHz, CDCl_3) δ 1.05 (6H, d, $J = 6.8$ Hz), 1.07 (6H, d, $J = 6.8$ Hz), 2.06–2.22 (2H, m), 2.64 (2H, t, $J = 7.8$ Hz), 3.00 (2H, t, $J = 7.8$ Hz), 3.67 (3H, s), 3.80 (2H, d, $J = 6.6$ Hz), 3.82 (2H, d, $J = 6.3$ Hz), 6.87 (1H, d, $J = 8.3$ Hz), 6.95 (2H, d, $J = 8.7$ Hz), 7.64 (1H, d, $J = 2.0$ Hz), 7.67 (1H, dd, $J = 8.3, 2.0$ Hz), 7.76 (2H, d, $J = 8.7$ Hz); MS m/z 413 ($\text{M} + \text{H}$) $^+$.

A mixture of **26** (10.4 g, 25.2 mmol) and 20 wt % aqueous NaOH (10.4 g) in acetone (30 mL) was stirred at 50 °C for 2 h before dilution with water (100 mL). The product that was precipitated by acidification to pH 1 with 12 M HCl was collected by filtration and washed with water (2×50 mL) to afford **4** (9.44 g, 94%) as a white solid, which was crystallized from CH_2Cl_2 /hexane to give colorless crystals, mp 102–103 °C: $^1\text{H NMR}$ (400 MHz, CDCl_3) δ 1.04 (6H, d, $J = 6.6$ Hz), 1.07 (6H, d, $J = 6.8$ Hz), 2.06–2.22 (2H, m), 2.71 (2H, t, $J = 7.7$ Hz), 3.00 (2H, t, $J = 7.7$ Hz), 3.80 (2H, d, $J = 6.4$ Hz), 3.82 (2H, d, $J = 6.6$ Hz), 6.87 (1H, d, $J = 8.5$ Hz), 6.95 (2H, d, $J = 8.8$ Hz), 7.66 (1H, d, $J = 2.2$ Hz), 7.69 (1H, dd, $J = 8.5, 2.2$ Hz), 7.76 (2H, d, $J = 8.8$ Hz); MS m/z 397 ($\text{M} - \text{H}$) $^-$. Anal. ($\text{C}_{24}\text{H}_{30}\text{O}_5$) C, H.

3-[2-Isobutoxy-5-(3-isobutoxybenzoyl)phenyl]propionic Acid (5). Compounds **22** and **25** were treated by the procedure described for **4** to afford **5** (85%) as a white solid, which was crystallized from CH_2Cl_2 /hexane to give colorless crystals, mp 77–78 °C: $^1\text{H NMR}$ (400 MHz, CDCl_3) δ 1.03 (6H, d, $J = 6.8$ Hz), 1.07 (6H, d, $J = 6.8$ Hz), 2.04–2.22 (2H, m), 2.70 (2H, t, $J = 7.7$ Hz), 3.00 (2H, t, $J = 7.7$ Hz), 3.77 (2H, d, $J = 6.4$ Hz), 3.83 (2H, d, $J = 6.3$ Hz), 6.87 (1H, d, $J = 9.3$ Hz), 7.10 (1H, dd, $J = 7.9, 2.6$ Hz),

7.22–7.32 (2H, m), 7.35 (1H, t, $J = 7.9$ Hz), 7.68–7.78 (2H, m); MS m/z 397 ($\text{M} - \text{H}$) $^-$. Anal. ($\text{C}_{24}\text{H}_{30}\text{O}_5$) C, H.

3-[3-(4-Isobutoxybenzoyl)phenyl]propionic Acid (6). Compound **20** and isobutoxybenzene were treated by the procedure described for **4** to afford **6** (77%) as a white solid, which was crystallized from CH_2Cl_2 /hexane to give colorless crystals, mp 98–99 °C: $^1\text{H NMR}$ (400 MHz, CDCl_3) δ 1.05 (6H, d, $J = 6.6$ Hz), 2.06–2.18 (1H, m), 2.73 (2H, t, $J = 7.7$ Hz), 3.03 (2H, t, $J = 7.7$ Hz), 3.80 (2H, d, $J = 6.6$ Hz), 6.95 (2H, d, $J = 8.8$ Hz), 6.91–6.98 (3H, m), 7.36–7.46 (2H, m), 7.54–7.64 (2H, m), 7.80 (2H, d, $J = 8.8$ Hz); MS m/z 327 ($\text{M} + \text{H}$) $^+$, 325 ($\text{M} - \text{H}$) $^-$. Anal. ($\text{C}_{20}\text{H}_{22}\text{O}_4$) C, H.

3-(5-Benzoyl-2-isobutoxyphenyl)propionic Acid (7). Compound **22** and benzoyl chloride were treated by the procedure described for **4** to afford **7** (40%) as a white solid, which was crystallized from CH_2Cl_2 /hexane to give colorless crystals, mp 95–97 °C: $^1\text{H NMR}$ (400 MHz, CDCl_3) δ 1.07 (6H, d, $J = 6.6$ Hz), 2.08–2.24 (1H, m), 2.71 (2H, t, $J = 7.7$ Hz), 3.00 (2H, t, $J = 7.7$ Hz), 3.83 (2H, d, $J = 6.3$ Hz), 6.88 (1H, d, $J = 8.3$ Hz), 7.44–7.52 (2H, m), 7.52–7.60 (1H, m), 7.68–7.80 (4H, m); MS m/z 327 ($\text{M} + \text{H}$) $^+$, 325 ($\text{M} - \text{H}$) $^-$. Anal. ($\text{C}_{20}\text{H}_{22}\text{O}_4$) C, H.

Methyl 3-[2-Hydroxy-5-(4-isobutoxybenzoyl)phenyl]propionate (28). A mixture of **26** (1.00 g, 2.42 mmol) and AlCl_3 (1.94 g, 14.5 mmol) in 1,2-dichloroethane (10 mL) was stirred under reflux for 8 h before cooling to room temperature. The mixture was diluted with 2-butanone (50 mL) and then poured into a mixture of ice (15 g) and 12 M HCl (15 mL). The organic layer separated was sequentially washed with 1 M HCl (2×10 mL), water (1×10 mL), and brine (1×10 mL), dried over MgSO_4 , and concentrated under reduced pressure. The residual solid was triturated with hexane (10 mL) to give **27** (0.55 g) as a pale red solid: $^1\text{H NMR}$ (400 MHz, $\text{DMSO}-d_6$) δ 2.85 (2H, t, $J = 7.3$ Hz), 3.08 (2H, t, $J = 7.3$ Hz), 6.90 (2H, d, $J = 8.7$ Hz), 7.19 (1H, d, $J = 8.3$ Hz), 7.59 (1H, dd, $J = 8.3, 2.2$ Hz), 7.65–7.67 (1H, m), 7.66 (2H, d, $J = 8.7$ Hz), 10.43 (1H, s); MS m/z 269 ($\text{M} + \text{H}$) $^+$, 267 ($\text{M} - \text{H}$) $^-$. To a suspension of **27** (0.55 g), isobutyl alcohol (0.18 g, 2.43 mmol), and triphenylphosphine (0.65 g, 2.48 mmol) in THF (6 mL) at temperatures below 40 °C was added dropwise DIAD (0.50 g, 2.47 mmol). After being stirred for 30 min, NaOMe (28 wt % in MeOH, 1.98 g, 10.3 mmol) was added dropwise to the ice-cooled mixture with stirring, and then the resulting mixture was stirred at room temperature for 30 min. The reaction mixture was treated with toluene (10 mL) and 1 M HCl (20 mL). The organic layer was sequentially washed with water (1×10 mL) and brine (1×10 mL), dried over MgSO_4 , and concentrated under reduced pressure. The residue was purified by chromatography (silica gel 100 g, 4:1 hexane/EtOAc) to give **28** (0.60 g, 69%) as a white solid: $^1\text{H NMR}$ (400 MHz, CDCl_3) δ 1.05 (6H, d, $J = 6.8$ Hz), 2.06–2.18 (1H, m), 2.76 (2H, t, $J = 6.3$ Hz), 2.95 (2H, t, $J = 6.3$ Hz), 3.72 (3H, s), 3.80 (2H, d, $J = 6.6$ Hz), 6.94 (1H, d, $J = 8.3$ Hz), 6.95 (2H, d, $J = 8.7$ Hz), 7.58 (1H, dd, $J = 8.3, 2.2$ Hz), 7.63 (1H, d, $J = 2.2$ Hz), 7.76 (2H, d, $J = 8.7$ Hz), 7.95 (1H, br s); MS m/z 357 ($\text{M} + \text{H}$) $^+$, 355 ($\text{M} - \text{H}$) $^-$.

Methyl 3-[2-Hydroxy-5-(4-propoxybenzoyl)phenyl]propionate (29). Compound **26** (1.00 g, 2.42 mmol) was treated by the procedure described for **28** except using *n*-propyl alcohol to afford **29** (0.56 g, 67%) as a white solid: $^1\text{H NMR}$ (400 MHz, CDCl_3) δ 1.06 (3H, t, $J = 7.3$ Hz), 1.80–1.90 (2H, m), 2.76 (2H, t, $J = 6.2$ Hz), 2.95 (2H, t, $J = 6.2$ Hz), 3.72 (3H, s), 4.00 (2H, t, $J = 6.6$ Hz), 6.94 (1H, d, $J = 8.4$ Hz), 6.95 (2H, d, $J = 8.8$ Hz), 7.57 (1H, dd, $J = 8.4, 2.1$ Hz), 7.63 (1H, d, $J = 2.1$ Hz), 7.76 (2H, d, $J = 8.8$ Hz), 7.92 (1H, s); MS m/z 341 ($\text{M} - \text{H}$) $^-$.

Methyl 3-[5-(4-Benzyloxybenzoyl)-2-hydroxyphenyl]propionate (30). Compound **26** (1.00 g, 2.42 mmol) was treated by the procedure described for **28** except using benzyl alcohol to afford **30** (0.66 g, 70%) as a white solid: $^1\text{H NMR}$ (400 MHz, CDCl_3) δ 2.76 (2H, t, $J = 6.2$ Hz), 2.95 (2H, t, $J = 6.2$ Hz), 3.72 (3H, s), 5.15 (2H, s), 6.94 (1H, d, $J = 8.4$ Hz), 7.03 (2H, d, $J = 8.9$ Hz), 7.32–7.48 (5H, m), 7.58 (1H, dd, $J = 8.4, 2.2$ Hz), 7.64 (1H, d, $J = 2.2$ Hz), 7.77 (2H, d, $J = 8.9$ Hz), 7.94 (1H, s); MS m/z 391 ($\text{M} + \text{H}$) $^+$, 389 ($\text{M} - \text{H}$) $^-$.

3-[5-(4-Isobutoxybenzoyl)-2-propoxyphenyl]propionic Acid (9). To a stirred suspension of **28** (3.00 g, 8.42 mmol) and K_2CO_3 (1.16 g, 8.39 mmol) in DMF (15 mL) at room temperature was added *n*-propyl bromide (1.55 g, 12.6 mmol), and the mixture was stirred at 90–100 °C for 1 h. After cooling to room temperature, the reaction mixture was treated with toluene (15 mL) and water (60 mL) followed by acidification to pH 4 with 6 M HCl. The organic layer was washed with water (1 × 20 mL) and brine (1 × 20 mL), dried over $MgSO_4$, and concentrated under reduced pressure. The residue was purified by chromatography (silica gel 75 g, 2:1 hexane/EtOAc) to give methyl 3-[5-(4-isobutoxybenzoyl)-2-propoxyphenyl]propionate (2.73 g, 81%) as a white solid: 1H NMR (400 MHz, $CDCl_3$) δ 1.02–1.12 (9H, m), 1.81–1.93 (2H, m), 2.00–2.20 (1H, m), 2.64 (2H, t, $J = 7.8$ Hz), 2.99 (2H, t, $J = 7.8$ Hz), 3.67 (3H, s), 3.80 (2H, d, $J = 6.3$ Hz), 4.02 (2H, t, $J = 6.3$ Hz), 6.87 (1H, d, $J = 8.4$ Hz), 6.95 (2H, d, $J = 8.7$ Hz), 7.64 (1H, d, $J = 2.2$ Hz), 7.67 (1H, dd, $J = 8.4, 2.2$ Hz), 7.77 (2H, d, $J = 8.7$ Hz); MS m/z 400 (M + H)⁺.

A mixture of the ester (1.00 g, 2.51 mmol) obtained above and 20 wt % aqueous NaOH (1.50 g) in acetone (4 mL) was stirred at 50 °C for 1 h before dilution with water (12 mL). The product that was precipitated by acidification to pH 1 with 6 M HCl was collected by filtration and washed with water (2 × 5 mL) to afford **9** (0.91 g, 94%) as a white crystalline solid, mp 107–108 °C: 1H NMR (400 MHz, $CDCl_3$) δ 1.04 (6H, d, $J = 6.6$ Hz), 1.07 (3H, t, $J = 7.4$ Hz), 1.80–1.94 (2H, m), 2.04–2.20 (1H, m), 2.71, 2.99 (each 2H, t, $J = 7.6$ Hz), 3.79 (2H, d, $J = 6.6$ Hz), 4.01 (2H, t, $J = 6.5$ Hz), 6.88 (1H, d, $J = 8.3$ Hz), 6.95 (2H, d, $J = 8.7$ Hz), 7.66 (1H, d, $J = 2.1$ Hz), 7.69 (1H, dd, $J = 8.3, 2.1$ Hz), 7.76 (2H, d, $J = 8.7$ Hz); MS m/z 383 (M - H)⁻. Anal. (C₂₃H₂₈O₅) C, H.

3-[2-Benzoyloxy-5-(4-isobutoxybenzoyl)phenyl]propionic Acid (11). Compound **28** was treated by the procedure described for **9** except using benzyl bromide to afford **11** (67%) as a white solid, which was crystallized from hexane/diisopropyl ether to give colorless crystals, mp 100 °C: 1H NMR (400 MHz, $CDCl_3$) δ 1.04 (6H, d, $J = 6.6$ Hz), 2.02–2.18 (1H, m), 2.72 (2H, t, $J = 7.6$ Hz), 3.04 (2H, t, $J = 7.6$ Hz), 3.79 (2H, d, $J = 6.6$ Hz), 5.17 (2H, s), 6.91–6.98 (3H, m), 7.30–7.48 (5H, m), 7.64–7.70 (2H, m), 7.76 (2H, d, $J = 8.8$ Hz); MS m/z 431 (M - H)⁻. Anal. (C₂₇H₂₈O₅) C, H.

3-[2-Isobutoxy-5-(4-propoxybenzoyl)phenyl]propionic Acid (10). Compound **29** was treated by the procedure described for **9** except using isobutyl bromide to afford **10** (85%) as a white crystalline solid, mp 128–129 °C: 1H NMR (400 MHz, $CDCl_3$) δ 1.00–1.12 (9H, m), 1.76–1.92 (2H, m), 2.08–2.24 (1H, m), 2.71 (2H, t, $J = 7.6$ Hz), 3.00 (2H, t, $J = 7.6$ Hz), 3.82 (2H, d, $J = 6.4$ Hz), 4.00 (2H, t, $J = 6.6$ Hz), 6.87 (1H, d, $J = 8.4$ Hz), 6.95 (2H, d, $J = 8.7$ Hz), 7.66 (1H, d, $J = 2.1$ Hz), 7.69 (1H, dd, $J = 8.4, 2.1$ Hz), 7.76 (2H, d, $J = 8.7$ Hz); MS m/z 383 (M - H)⁻. Anal. (C₂₃H₂₈O₅) C, H.

3-[5-(4-Benzoyloxybenzoyl)-2-isobutoxyphenyl]propionic Acid (12). Compound **30** was treated by the procedure described for **9** except using isobutyl bromide to afford **12** (79%) as a white solid, which was crystallized from CH_2Cl_2 /hexane to give colorless crystals, mp 150–151 °C: 1H NMR (400 MHz, $CDCl_3$) δ 1.06 (6H, d, $J = 6.6$ Hz), 2.08–2.20 (1H, m), 2.71 (2H, t, $J = 7.7$ Hz), 3.00 (2H, t, $J = 7.7$ Hz), 3.82 (2H, d, $J = 6.3$ Hz), 5.15 (2H, s), 6.87 (1H, d, $J = 8.3$ Hz), 7.03 (2H, d, $J = 8.7$ Hz), 7.30–7.48 (5H, m), 7.60–7.72 (2H, m), 7.77 (2H, d, $J = 8.7$ Hz); MS m/z 432 (M - H)⁻. Anal. (C₂₇H₂₈O₅) C, H.

Bis(4-isobutoxyphenyl)methanone (8). To a stirred suspension of bis(4-hydroxyphenyl)methanone (2.00 g, 9.34 mmol) and K_2CO_3 (3.87 g, 28.0 mmol) in DMF (20 mL) at room temperature was added isobutyl bromide (3.84 g, 28.0 mmol), and then the mixture was heated with stirring at 100 °C for 1 h. Additional K_2CO_3 (1.29 g, 9.33 mmol) and isobutyl bromide (1.28 g, 9.34 mmol) were then added, and the heating was continued for a further 1.5 h. The reaction mixture was cooled to room temperature before filtration, and the residue was rinsed with EtOAc (3 × 30 mL). The filtrate was treated with water (50 mL) followed by acidification to pH 2 with 6 M HCl, and the aqueous layer separated was

extracted with EtOAc (1 × 30 mL). The combined organic extracts were washed with water (1 × 30 mL) and brine (1 × 30 mL), followed by the addition of $CHCl_3$ (30 mL). The solution was dried over $MgSO_4$ and concentrated under reduced pressure. The residue was triturated with hexane (20 mL) to afford **8** (2.88 g, 94%) as a white solid, which was crystallized from CH_2Cl_2 /hexane to give colorless crystals, mp 118–119 °C: 1H NMR (400 MHz, $CDCl_3$) δ 1.05 (12H, d, $J = 6.8$ Hz), 2.04–2.20 (2H, m), 3.80 (4H, d, $J = 6.6$ Hz), 6.95 (4H, d, $J = 8.5$ Hz), 7.77 (4H, d, $J = 8.5$ Hz); MS m/z 327 (M + H)⁺. Anal. (C₂₁H₂₆O₃) C, H.

3-[2-Isobutoxy-5-(4-isobutoxybenzoyl)phenyl]propionamide (13). To a stirred solution of **4** (5.00 g, 12.5 mmol) in THF (50 mL) at room temperature was sequentially added oxalyl chloride (1.91 g, 15.0 mmol) and DMF (50 μ L), and the mixture was stirred for 3 h. The resulting mixture was slowly poured into ice-cooled 25 wt % NH_4OH (50 mL) with vigorous stirring. After being stirred at 5 °C for 30 min, the mixture was adjusted to pH 6 with 6 M HCl and extracted with EtOAc (1 × 100 mL). The aqueous layer separated was extracted with EtOAc (1 × 50 mL), and the organic extracts were washed with water (1 × 50 mL) and brine (1 × 50 mL), dried over $MgSO_4$, and concentrated under reduced pressure. The residual solid was triturated with hexane (100 mL) to afford **13** (4.67 g, 94%) as a white solid, which was crystallized from CH_2Cl_2 /hexane to give colorless crystals, mp 123 °C: 1H NMR (400 MHz, $CDCl_3$) δ 1.05 (6H, d, $J = 6.8$ Hz), 1.08 (6H, d, $J = 6.6$ Hz), 2.06–2.22 (2H, m), 2.56 (2H, t, $J = 7.7$ Hz), 3.02 (2H, t, $J = 7.7$ Hz), 3.80 (2H, d, $J = 6.6$ Hz), 3.83 (2H, d, $J = 6.3$ Hz), 5.29 (1H, br s), 5.38 (1H, br s), 6.88 (1H, d, $J = 8.1$ Hz), 6.95 (2H, d, $J = 8.5$ Hz), 7.62–7.70 (2H, m), 7.76 (2H, d, $J = 8.5$ Hz); MS m/z 399 (M + H)⁺. Anal. (C₂₄H₃₁NO₄) C, H, N.

ELISA-Based AP-1 Binding Assay: Preparation of c-Fos and c-Jun bZIP Peptides. The resin and all of the protected amino acids and coupling reagents were purchased from Watanabe Chemical Industries (Hiroshima, Japan). All of the reagents and solvents were reagent grade or better and were used without further purification. High-performance liquid chromatography (HPLC) was performed using a Hitachi L-7100 apparatus equipped with an L-7400 UV detector (peak detection at 230 nm) and a PROTEINE-RP column (YMC-Pack, YMC Co., Kyoto, Japan) of 250 × 20 mm for preparative HPLC or 150 × 4.6 mm for analytical HPLC. c-Jun bZIP peptide [c-Jun (263–324) Cys278Ser] and biotinylated c-Fos bZIP peptide [*N*-biotinyl-(Gly)₄-c-Fos (139–200) Cys154Ser]⁵ were synthesized manually using standard solid-phase peptide chemistry with *tert*-butoxycarbonyl (Boc)-protected amino acids on Boc-His(benzyloxymethyl)-PAM resin²⁴ at a 0.30 mmol scale. The Boc protecting group was removed by treatment with trifluoroacetic acid (10 mL) at room temperature for 3 min. Coupling with Boc-protected amino acids (4 equiv) was then performed in the presence of *N,N*-diisopropylethylamine (6 equiv) and 2-(1*H*-benzotriazol-1-yl)-1,1,3,3-tetramethyluronium hexafluorophosphate (3.8 equiv) in *N*-methyl-2-pyrrolidone (8 mL) at room temperature for 30 min.²⁵ Subsequently, the peptide resin was treated with decanoic anhydride (0.3 mol/L in 1:1 DMF/ CH_2Cl_2 , 10 mL) at room temperature for 30 min. The protected c-Jun bZIP peptide resin (0.50 g) was treated with a reagent containing anhydrous HF (1.5 mL) and dimethyl sulfide (4.5 mL) with stirring at 0 °C for 1.5 h to remove the remaining O- and N-protecting groups.²⁶ After the evaporation of HF, ether was added to the resin, which was then filtered, washed in CH_2Cl_2 (5 × 10 mL), followed by dried in vacuo. The resin was treated with a reagent containing anhydrous HF (4.5 mL) and *p*-cresol (1.5 mL) with stirring at 0 °C for 1.5 h to induce cleavage of the peptide from the resin. The precipitate was collected by centrifugation and dissolved in water. The exhausted resin was filtered, and the filtrate was purified by reverse phase HPLC eluted with a linear gradient of acetonitrile in water containing 0.1% trifluoroacetic acid at a flow rate of 7.0 mL/min before lyophilization. Biotinylated c-Fos bZIP peptide was synthesized according to the procedure that was used to prepare the c-Jun bZIP peptide.

The peptides were separately dissolved in 20 mM Tris-HCl buffer (pH 7.5) containing 50 mM KCl, 1 mM ethylenediaminetetraacetic acid (EDTA), 10 mM $MgCl_2$, 1 mM dithiothreitol (DTT), 0.5 M

guanidine HCl, and 30% glycerol. Equimolar quantities of both of the solutions were mixed together and the resulting mixture was used as the AP-1 bZIP peptide.

Binding Assay of AP-1 bZIP Peptide and AP-1 Double-Stranded Oligonucleotides. The inhibitory activities of the synthetic compounds on the DNA-binding activity of AP-1 were evaluated using an ELISA-based AP-1 binding assay with synthetic double-stranded oligonucleotides that contained the AP-1 binding site (shown in bold) and the AP-1 bZIP peptide. The AP-1 bZIP peptide (10 pmol/well) was added to an avidin-coated 96-well ELISA plate, washed, and then blocked with bovine serum albumin. Digoxigenin-labeled double-stranded oligonucleotides (22-mer) containing an AP-1 binding sequence (5'-CTAGT**GATGAGT-CAGCCG**GATC-3' and 5'-GATCC**GGCTGACTCAT**CTACTAG-3') (Nisshinbo Industries, Inc., Tokyo, Japan) were reacted in the presence or absence of each sample at room temperature for 1 h in a binding reaction solution [25 mM Tris-HCl (pH 7.9) containing 0.5 mM EDTA, 0.05% Nonidet P-40 and 10% glycerol]. Subsequently, the unbound labeled oligonucleotide was washed out with HEPES-KOH (pH 7.9) buffer containing 0.5 mM EDTA, 50 mM KCl, 10% glycerol, 0.1% BSA, and 0.05% Tween-20. The peroxidase-conjugated anti-digoxigenin antibody (Roche Diagnostics, Indianapolis, IN) was then added and reacted with the labeled oligonucleotide bound to AP-1. After washing out the excess antibody with HEPES-KOH buffer containing 0.05% Tween-20, the residue was reacted for a predetermined period of time in 100 mM citrate buffer (pH 5.0) containing 0.03% H₂O₂ using *o*-phenylenediamine as a substrate. After adding sulfuric acid solution to each well, the absorbance at 492 nm was measured with a Microplate spectrophotometer (Bio-Rad Laboratories, Hercules, CA). Taking the absorbance in the absence of sample as 100%, the inhibition rate of each sample was calculated from the absorbance in the presence of the sample. The IC₅₀ values were calculated based on a logistic concentration-response curve using the SAS system version 8.2 (SAS Institute, Cary, NC).

Cell-Based Assay: Plasmids. Reporter plasmids containing the firefly luciferase reporter gene driven by a basic promoter element (TATA box) plus a defined inducible cis-enhancer element were utilized (PathDetect in Vivo Signal Transduction Pathway *cis*-Reporting Systems, Stratagene, La Jolla, CA). The firefly luciferase gene in the reporter plasmid (pAP-1-Luc) was controlled by synthetic enhancer sequences comprising seven repeats of the binding sites for AP-1; TGACTAA. A control plasmid expressing *Renilla reniformis* luciferase driven by the herpes simplex virus thymidine kinase promoter, pRL-TK Vector (Promega, Madison, WI), was used to correct the efficiency of transfection.

Cell Culture. The murine fibroblast cell line NIH3T3 was obtained from the American Type Culture Collection (ATCC No. CRL-1658; Rockville, MD) and grown in Dulbecco's modified Eagle's medium (DMEM; Nissui Pharmaceutical, Tokyo, Japan) supplemented with 4 mM l-glutamine (Wako Pure Chemical, Osaka, Japan), 1.5 g/L glucose (Wako Pure Chemical), 10% heat-inactivated fetal calf serum (FCS; JRH Biosciences, Lenexa, KS), and 60 µg/mL kanamycin sulfate (Sigma-Aldrich, St. Luis, MO) at 37 °C and 5% CO₂.

Transient Transfection and Reporter Gene Assay. Approximately 1 × 10⁴ cells in 100 µL of 10% FCS-DMEM were plated into a 96-well tissue culture plate (Iwaki Glass, Chiba, Japan) 24 h before transfection (day 0). On day 1, the cells in each well were transiently cotransfected with 40 ng of pAP-1-Luc plasmid and 4 ng of pRL-TK Vector using the FuGENE 6 transfection reagent (Roche Diagnostics, Indianapolis, IN). After transfection for 6 h at 37 °C, the cells were cultured in 0.5% FCS-DMEM. On day 2, the medium was exchanged with 0.5% FCS-DMEM containing the compounds. After 1 h, phorbol 12-myristate 13-acetate (TPA) was added to each well (100 ng/mL). Three hours after TPA stimulation, whole cell lysates were examined for luciferase activity (Dual-Luciferase Reporter Assay System, Promega) with a luminometer (Luminous CT-9000D; DIA-IATRON,

Tokyo, Japan) according to the manufacturer's protocol. The firefly luciferase activity was normalized for transfection efficiency based on the Renilla luciferase activity. Taking the activity in the absence of sample as 100%, the inhibition rate of each sample was calculated from the absorbance in the presence of the sample. The IC₅₀ values were calculated based on a logistic concentration-response curve using the SAS system version 8.2.

Acknowledgment. This study was partially supported by the Japan Science and Technology Agency.

Supporting Information Available: Characterization data for esters of compounds 5–7 and 10–12 plus elemental analysis data for compounds 2–13. This material is available free of charge via the Internet at <http://pubs.acs.org>.

References

- (1) Angel, P.; Karin, M. The Role of Jun, Fos and the AP-1 Complex in Cell-Proliferation and Transformation. *Biochim. Biophys. Acta* **1991**, *1072*, 129–157.
- (2) Wagner, E. F. AP-1 – Introductory Remarks. *Oncogene* **2001**, *20*, 2334–2335.
- (3) Shiozawa, S.; Shimizu, K.; Tanaka, K.; Hino, K. Studies on the Contribution of c-fos/AP-1 to Arthritic Joint Destruction. *J. Clin. Invest.* **1997**, *99*, 1210–1216.
- (4) Suto, M. J.; Ransone, L. J. Novel Approaches for the Treatment of Inflammatory Diseases: Inhibitors of NF-κB and AP-1. *Curr. Pharm. Des.* **1997**, *3*, 515–528.
- (5) Glover, J. N. M.; Harrison, S. C. Crystal Structure of the Heterodimeric bZIP Transcription Factor c-Fos-c-Jun Bound to DNA. *Nature* **1995**, *373*, 257–261.
- (6) Hahm, E.-R.; Cheon, G.; Lee, J.; Kim, B.; Park, C.; Yang, C.-H. New and Known Symmetrical Curcumin Derivatives Inhibit the Formation of Fos-Jun-DNA Complex. *Cancer Lett.* **2002**, *184*, 89–96.
- (7) Park, S.; Lee, D.-K.; Yang, C.-H. Inhibition of Fos-Jun-DNA Complex Formation by Dihydroguaiaretic Acid and In Vitro Cytotoxic Effects on Cancer Cells. *Cancer Lett.* **1998**, *127*, 23–28.
- (8) Goto, M.; Masegi, M.; Yamauchi, T.; Chiba, K.; Kuboi, Y.; Harada, K.; Naruse, N. K1115 A, a New Anthraquinone Derivative that Inhibits the Binding of Activator Protein-1 (AP-1) to its Recognition Sites. *J. Antibiot.* **1998**, *51*, 539–544.
- (9) Tsuchida, K.; Chaki, H.; Takakura, T.; Yokotani, J.; Aikawa, Y.; Shiozawa, S.; Gouda, H.; Hirono, S. Design, Synthesis, and Biological Evaluation of New Cyclic Disulfide Decapeptides That Inhibit the Binding of AP-1 to DNA. *J. Med. Chem.* **2004**, *47*, 4239–4246.
- (10) Olson, G. L.; Bolin, D. R.; Bonner, M. P.; Bös, M.; Cook, C. M.; Fry, D. C.; Graves, B. J.; Hatada, M.; Hill, D. E.; Kahn, M.; Madison, V. S.; Rusiecki, V. K.; Sarabu, R.; Sepinwall, J.; Vincent, G. P.; Voss, M. E. Concepts and Progress in the Development of Peptide Mimetics. *J. Med. Chem.* **1993**, *36*, 3039–3049.
- (11) Gante, J. Peptidomimetics—Tailored Enzyme Inhibitors. *Angew. Chem., Int. Ed. Engl.* **1994**, *33*, 1699–1720.
- (12) Hruby, V. J.; Balse, P. M. Conformational and Topographical Considerations in Designing Agonist Peptidomimetics from Peptide Leads. *Curr. Med. Chem.* **2000**, *7*, 945–970.
- (13) Cramer, R. D.; Jilek, R. J.; Guessregen, S.; Clark, S. J.; Wendt, B.; Clark, R. D. “Lead Hopping”. Validation of Topomer Similarity as a Superior Predictor of Similar Biological Activities. *J. Med. Chem.* **2004**, *47*, 6777–6791.
- (14) Schneider, G.; Böhm, H.-J. Virtual Screening and Fast Automated Docking Methods. *Drug Discovery Today* **2002**, *7*, 64–70.
- (15) Honma, T.; Hayashi, K.; Aoyama, T.; Hashimoto N.; Machida T.; Fukasawa K.; Iwama T.; Ikeura C.; Ikuta M.; Suzuki-Takahashi I.; Iwasawa Y.; Hayama T.; Nishimura S.; Morishima H. Structure-Based Generation of a New Class of Potent Cdk4 Inhibitors: New de Novo Design Strategy and Library Design. *J. Med. Chem.* **2001**, *44*, 4615–4627.
- (16) Schneider, G.; Fechner, U. Computer-Based *De Novo* Design of Drug-Like Molecules. *Nat. Rev. Drug Discovery* **2005**, *4*, 649–663.
- (17) Nyburg, S. C. Some Uses of a Best Molecular Fit Routine. *Acta Crystallogr.* **1974**, *B30* (part D), 251–253.
- (18) Oya, M.; Baba, T.; Kato, E.; Kawashima, Y.; Watanabe, T. Synthesis and Antihypertensive Activity of *N*-(Mercaptoacyl)-thiazolidinecarboxylic Acids. *Chem. Pharm. Bull.* **1982**, *30*, 440–461.
- (19) Smith, R. A. Studies in the Rearrangements of Phenyl Ethers. The Action of Aluminum Chloride on Butyl Phenyl Ethers. *J. Am. Chem. Soc.* **1933**, *55*, 3718–3721.

- (20) Schuda, P. F.; Price, W. A. Total Synthesis of Isoflavones: Jamaicin, Calopogonium Isoflavone-B, Pseudobaptigenin, and Maxima Substance-B. Friedel–Crafts Acylation Reactions with Acid-Sensitive Substrates. *J. Org. Chem.* **1987**, *52*, 1972–1979.
- (21) Dalcanale, E.; Montanari, F. Selective Oxidation of Aldehydes to Carboxylic Acids with Sodium Chlorite-Hydrogen Peroxide. *J. Org. Chem.* **1986**, *51*, 567–569.
- (22) SYBYL 6.5; Tripos, Inc.: St. Louis, MO, 1998.
- (23) Halgren, T. A. Merck Molecular Force Field. I. Basis, Form, Scope, Parameterization, and Performance of MMFF94. *J. Comput. Chem.* **1996**, *17*, 490–519.
- (24) Mitchell, A. R.; Erickson, B. W.; Ryabtsev, M. N.; Hodges, R. S.; Merrifield, R. B. *tert*-Butoxycarbonylaminoacyl-4-(oxymethyl)-phenylacetamidomethyl-Resin, a More Acid-Resistant Support for Solid-Phase Peptide Synthesis. *J. Am. Chem. Soc.* **1976**, *98*, 7357–7362.
- (25) Knorr, R.; Trzeciak, A.; Bannwarth, W.; Gillessen, D. New Coupling Reagents in Peptide Chemistry. *Tetrahedron Lett.* **1989**, *30*, 1927–1930.
- (26) Tam, J. P.; Heath, W. F.; Merrifield, R. B. S_N2 Deprotection of Synthetic Peptides with a Low Concentration of HF in Dimethyl Sulfide: Evidence and Application in Peptide Synthesis. *J. Am. Chem. Soc.* **1983**, *105*, 6442–6455.

JM050550D